THE JOURNAL OF BIOLOGICAL CHEMISTRY VOL. 284, NO. 6, pp. 3842–3854, February 6, 2009

Functional Significance of E_2 State Stabilization by Specific α/β-Subunit Interactions of Na,K- and H,K-ATPase*[S]

Received for publication, October 22, 2008, and in revised form, November 24, 2008 Published, JBC Papers in Press, December 8, 2008, DOI 10.1074/jbc.M808101200

Katharina L. Dürr[‡1], Neslihan N. Tavraz[‡], Robert E. Dempski[§], Ernst Bamberg[§¶], and Thomas Friedrich[‡]

From the [‡]Technical University of Berlin, Institute of Chemistry, D-10623 Berlin, Germany, the [§]Max Planck Institute of Biophysics, Department of Biophysical Chemistry, D-60438 Frankfurt/Main, Germany, and the [¶]Johann Wolfgang Goethe University Frankfurt, Chemical and Pharmaceutical Sciences Department, D-60439 Frankfurt/Main, Germany

The β-subunits of Na,K-ATPase and H,K-ATPase have important functions in maturation and plasma membrane targeting of the catalytic α-subunit but also modulate the transport activity of the holoenzymes. In this study, we show that tryptophan replacement of two highly conserved tyrosines in the transmembrane domain of both Na,K- and gastric H,K-ATPase β-subunits resulted in considerable shifts of the voltage-dependent E_1P/E_2P distributions toward the E_1P state as inferred from presteady-state current and voltage clamp fluorometric measurements of tetramethylrhodamine-6-maleimide-labeled ATPases. The shifts in conformational equilibria were accompanied by significant decreases in the apparent affinities for extracellular K^+ that were moderate for the Na,K-ATPase β-(Y39W,Y43W) mutation but much more pronounced for the corresponding H,K-ATPase β-(Y44W,Y48W) variant. Moreover in the Na,K-ATPase β-(Y39W,Y43W) mutant, the apparent rate constant for reverse binding of extracellular Na^+ and the subsequent E_2P-E_1P conversion, as determined from transient current kinetics, was significantly accelerated, resulting in enhanced Na^+ competition for extracellular K^+ binding especially at extremely negative potentials. Analogously the reverse binding of extracellular protons and subsequent E_2P-E_1P conversion was accelerated by the H,K-ATPase β-(Y44W,Y48W) mutation, and H^+ secretion was strongly impaired. Remarkably tryptophan replacements of residues in the M7 segment of Na,K- and H,K-ATPase α-subunits, which are at interacting distance to the β-tyrosines, resulted in similar E_1 shifts, indicating their participation in stabilization of E_2. Thus, interactions between selected residues within the transmembrane regions of α- and β-subunits of P_{2C}-type ATPases exert an E_2-stabilizing effect, which is of particular importance for efficient H^+ pumping by H,K-ATPase under *in vivo* conditions.

The ubiquitous sodium pump and the closely related gastric proton pump are members of the P-type ATPase family that comprises more than 200 identified members (1, 2). Apart from the highly homologous Na,K-ATPase α-isoforms, the catalytic subunits of Na,K-ATPase and H,K-ATPase share the highest sequence identity in the whole family (of about 62% between Na,K-ATPase α_1-subunit and gastric H,K-ATPase α-subunit (3)). Besides the bacterial Kdp-ATPase, which is composed of four essential subunits (4), Na,K- and H,K-ATPases are the only P-type ATPase family members that require an additional β-subunit for folding, membrane insertion, and plasma membrane delivery of the catalytically active α-subunits (5–7). With only 20–30% overall sequence identity the three Na,K-ATPase β-subunit isoforms and the H,K-ATPase β-subunits from difference species are much less conserved than the α-subunits. However, all known β-subunits share the same basic overall structure: a short intracellular N-terminal domain followed by a single transmembrane span and a large C-terminal ectodomain, which contains highly conserved glycosylation sites and disulfide bridge-forming cysteine residues.

Because a unique feature of the oligomeric members of the P-type ATPase family is the ability to transport K^+ ions, it was speculated (8) that some structural particularities in the α-subunit that are required for potassium transport may be detrimental for proper folding and membrane integration and that the negative influence on these critical processes is overcome by the association with accessory subunits. In addition to this chaperone-like function, the β-subunit is essential for enzyme activity (9) and influences the transport properties of mature sodium and proton pumps. The existence of various tissue-specific Na,K-ATPase β-subunit isoforms, which result in holoenzymes with different cation affinities (10, 11), and the fact that Na,K-ATPase α-subunits co-expressed with H,K-ATPase β-subunits form active pumps (12), albeit with altered ion affinities (10, 13), strongly suggest a modulatory function of the β-subunit for ion translocation.

Results from several studies indicate that it is mainly the C-terminal extracellular domain of the β-subunit that modulates cation transport. For example, reduction of the disulfide bonds in the ectodomain of the β-subunit impairs the function of purified Na,K- or H,K-ATPase. Because this was prevented in the presence of cations (14–16), a potential role of the β-subunit in K^+ occlusion has been suggested. Functional analysis of chimeras between Na,K- and H,K-ATPase β-subunits confirmed that mostly α-β ectodomain interactions are responsible for the observed effects of the β-subunit on cation affinity

* This work was supported by the Max-Planck-Gesellschaft zur Förderung der Wissenschaften e.V. and the Deutsche Forschungsgemeinschaft (Grants SFB 472 and SFB 740 and Cluster of Excellence "Unifying Concepts in Catalysis"). The costs of publication of this article were defrayed in part by the payment of page charges. This article must therefore be hereby marked "*advertisement*" in accordance with 18 U.S.C. Section 1734 solely to indicate this fact.

[S] The on-line version of this article (available at http://www.jbc.org) contains supplemental Figs. 1 and 2 and Table 1.

[1] To whom correspondence should be addressed: Technical University of Berlin, Inst. of Chemistry, PC-14, Strasse des 17 Juni 135, D-10623 Berlin, Germany. Tel.: 49-30-31423511; Fax: 49-30-31478600; E-mail: Katharina.Duerr@TU-Berlin.DE.

and occlusion of the sodium pump (17–19). This is also in line with the electron density of the first 10–15 residues of the ectodomain, which was tentatively traced in the recent x-ray structure of the pig Na,K-ATPase holoenzyme (20) and clearly indicates that the extracellular M5/M6 and M7/M8 loops of the α-subunit are covered by a "lid" formed by the ectodomain of the β-subunit as suggested previously (15).

Yet not only ectodomain modifications have been shown to alter the transport properties. N-terminal truncation of the cytoplasmic domain of the β-subunit of the Na,K-ATPase resulted in changes of the apparent K^+ (19, 21) and Na^+ affinities (19) and affected the conformational equilibrium (22). Likewise an inhibitory antibody, which recognizes an epitope within the first 36 N-terminal amino acids of the β-subunit of H,K-ATPase (23), altered the K^+ affinity. However, cytoplasmic interactions are probably not directly responsible for the functional effects of β-subunits on cation binding of the sodium pump because, in contrast to a complete truncation, deletions or multiple mutational alterations of the N terminus did not affect the K^+ activation of Na,K-ATPase expressed in *Xenopus* oocytes (19). Furthermore results from a glycosylation mapping assay indicated a repositioning of the transmembrane segment as a consequence of the N-terminal truncation (24). This in turn may also impair the conformation of the ectodomain, whose significance for cation occlusion has already been outlined above. Even the observed repositioning of the transmembrane domain (TMD)[2] itself could be responsible for the reported K^+ effects in the N-terminally truncated β-variant because mutations in the TMD have also been shown to modify cation transport: tryptophan scanning mutagenesis in the TMD of the Na,K-ATPase β-subunit revealed that the replacement of two tyrosines by tryptophan has distinct and additive consequences for the cation affinities of the holoenzyme (25). Interestingly these tyrosines are highly conserved; they are actually present in all known β-subunits (represented by *red capital letters* in the β-TMD alignment shown in Fig. 1*C*). The apparent $K_{½}$ for extracellular K^+ activation of pump currents in *Xenopus* oocytes was significantly increased for a simultaneous tryptophan replacement of the two tyrosines in various β-subunit isoforms. Of note, this was accompanied by an increase of the apparent affinity for intracellular sodium and a reduced sensitivity toward the E_2-specific inhibitor vanadate. Therefore, it was concluded that the affinity changes might occur secondarily to a conformational, *i.e.* E_2-destabilizing, effect of the β-subunit mutations (25). However, direct evidence for a shift in the E_1P/E_2P distribution of the enzyme has not been provided yet. Given the high propensity of native gastric H,K-ATPase to occur in the E_2 state (26), which has been speculated to be of primary importance for efficient H^+ delivery to the luminal fluid against a 10^6-fold H^+ gradient *in vivo*, it is of high interest to identify possible interaction sites on the β- and ultimately also on the transmembrane domains of the α-subunit that are crucial for this unique E_2-specific structural stabilization.

In the current study we set out to identify molecular determinants of E_2-specific intersubunit interactions and utilized the technique of voltage clamp fluorometry (VCF) to directly determine the distribution between E_1 and E_2 states of wild type and mutated Na,K- and H,K-ATPase enzymes (27, 28). Because this method can be applied to the electrogenic Na,K-ATPase as well as to the electroneutrally operating gastric H,K-ATPase (29, 30), whether mutation of the conserved tyrosines causes similar conformational shifts in both enzymes can be investigated. Evidence is provided that the observed conformational effects are of a more general significance for ion translocation by oligomeric P-type ATPases. Furthermore we compared for both enzymes the effects of these β-subunit mutations on apparent cation affinities, which occur in conjunction with shifts in the distribution of E_1P/E_2P conformational states. Moreover we studied the effect of mutations of selected residues in the TMD7 of the Na,K- and H,K-ATPase α-subunit that are at interacting distance to the two β-subunit tyrosines (Fig. 1*B*). This strategy provided novel insights about the molecular details of interactions between β- and α-subunit transmembrane domains of oligomeric P_{2C}-type ATPases that are responsible for stabilization of the E_2 conformational state.

EXPERIMENTAL PROCEDURES

Molecular Biology—The cDNAs of the sheep Na,K-ATPase $β_1$-subunit, rat H,K-ATPase β-subunit, rat gastric H,K-ATPase α-subunit, and a modified form of the sheep Na,K-ATPase $α_1$-subunit without extracellularly exposed cysteine residues (containing mutations C911S and C964A (31)) and with reduced ouabain sensitivity in the millimolar range (achieved by the mutations Q111R and N122D (32)) were subcloned into vector pTLN (33) as described previously (27, 28). The reduced ouabain sensitivity of the latter construct allows selective inhibition of the endogenous *Xenopus* Na,K-ATPase and was therefore used for all co-expression studies with mutated $β_1$-constructs or as template for site-directed mutagenesis of the Na,K-ATPase α-subunit. Furthermore to exclude any background signals in voltage clamp fluorometric studies that could possibly arise from Na,K-ATPase enzymes assembled from heterologously expressed α-subunits and endogenous β-subunits we utilized the $β_1$-subunit sequence variant S62C for mutagenesis. The introduced cysteine is close to the transmembrane/extracellular interface and has been shown to give rise to voltage-dependent fluorescence changes upon site-directed fluorescence labeling with tetramethylrhodamine-6-maleimide (TMRM) without impairing enzyme function (28). To enable voltage clamp fluorometry on gastric H,K-ATPase, we co-expressed the wild type (or mutated) H,K-ATPase β-subunits with a modified H,K-ATPase α-subunit with a single cysteine replacement of a serine in the M5/M6 extracellular loop (S806C) that is homologous to the N790C mutation in the M5/M6 loop of the Na,K-ATPase α-subunit (28) and thus also suited for environmentally sensitive TMRM labeling (29). Rubidium uptake measurements confirmed that the S806C mutation did not affect the transport properties of H,K-ATPase (30). This construct was therefore used as a template for site-directed

[2] The abbreviations used are: TMD, transmembrane domain; TMRM, tetramethylrhodamine-6-maleimide; VCF, voltage clamp fluorometry; wt, wild type; MES, 2-(*N*-morpholino)ethanesulfonic acid; TMACl, tetramethylammonium chloride; MOPS, 3-(*N*-morpholino)propanesulfonic acid.

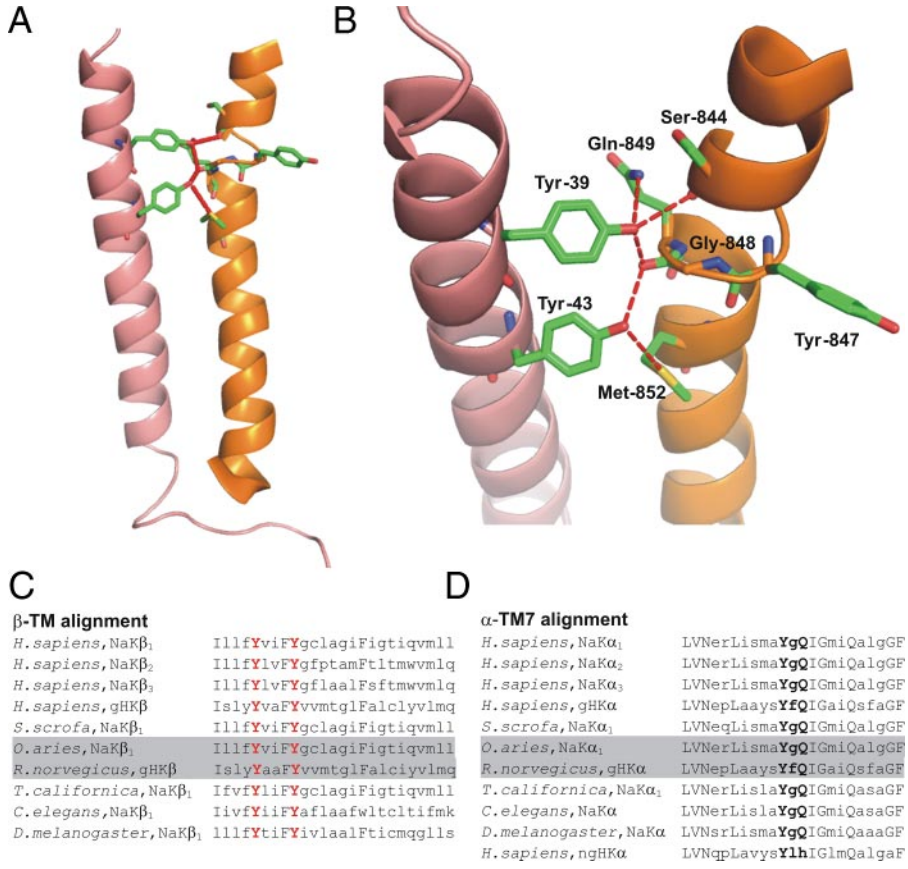

FIGURE 1. **Structural representation of the transmembrane α/β interface of pig renal Na,K-ATPase and alignments of α-TMD7 and β-TMD of several Na,K- and H,K-ATPases.** *A* and *B*, illustration of possible interaction sites between β-TMD (*pink*) and α-TMD7 (*orange*) of Na,K-ATPase according to the crystal structure (Protein Data Bank code 3B8E (20)). Putative hydrogen bonds are shown to a cutoff value of 3.8 Å. *B*, a close-up view of the β-TMD/α-TMD7 interface showing the two conserved tyrosines Tyr^{39} and Tyr^{43} of the β-subunit and some selected α-subunit residues located at interacting distance. *C* and *D*, alignments of the β-subunit TMD (*C*) and α-subunit TMD7 (*D*) of Na,K- and H,K-ATPases from different species or of different human isoforms. Highly conserved amino acids (in at least 75% of the investigated sequences according to manually refined alignments performed by Axelsen and Palmgren (2)) are represented by *capital letters*; residues altered by mutagenesis in the current study are shown in *bold letters*. The sheep α_1/β_1 Na,K-ATPase and the rat gastric H,K-ATPase used here are highlighted in *gray*. *NaK*, Na,K-ATPase; *gHK*, gastric H,K-ATPase; *ngHK*, non-gastric H,K-ATPase. *Homo sapiens*, *Sus scrofa*, *Ovis aries*, *Rattus norvegicus*, *Torpedo californica*, *Caenorhabditis elegans*, and *Drosophila melanogaster* are shown.

mutagenesis to introduce mutations in TMD7 of the H,K-ATPase α-subunit. All mutations were done using the QuikChange multi site-directed mutagenesis kit (Stratagene) and verified by DNA sequencing.

Oocyte Preparation and cRNA Injection—*Xenopus* oocytes were obtained by collagenase treatment after partial ovariectomy from *Xenopus laevis* females. cRNAs were prepared using the SP6 mMessage mMachine kit (Ambion, Austin, Texas). A 50-nl aliquot containing 20–25 ng of Na,K-ATPase and 1.5–2.5 ng of Na,K-ATPase β_1-subunit cRNA (or 20–25 ng of H,K-ATPase α-subunit cRNA and 5 ng of H,K-ATPase β-subunit) were injected into each cell. After injection, oocytes were kept in ORI buffer (110 mM NaCl, 5 mM KCl, 2 mM $CaCl_2$, 5 mM HEPES, pH 7.4) containing 50 mg/liter gentamycin at 18 °C for 3–5 and 2 days for the Na,K-ATPase and H,K-ATPase, respectively.

Isolation of Plasma Membranes from X. laevis Oocytes—The isolation of plasma membranes was carried out using positively charged silica beads as described by Kamsteeg and Deen (35), who reported a 25- or 450-fold higher yield with this technique compared with standard isolation or biotinylation procedures. Moreover because binding of these beads is carried out on intact oocytes, a high purity of the plasma membrane fraction is achieved with only minor contaminations by internal membranes (36).

After removal of their follicular cell layer, 8–12 oocytes were rotated in 1% colloidal silica (Ludox Cl, Sigma-Aldrich) in MES-buffered saline for silica (MBSS; 20 mM MES, 80 mM NaCl, pH 6.0) for 30 min at 4 °C. After washing two times in MBSS, the oocytes were rotated at 4 °C in 0.1% polyacrylic acid (Sigma-Aldrich) in MBSS for 30 min. This blocking agent is added to coat unbound beads and solvent-exposed surfaces of beads that were already bound to oocytes. Afterward the oocytes were washed two times in modified Barth's solution (MBS; 0.33 mM $Ca(NO_3)_2$, 0.41 mM $CaCl_2$, 88 mM NaCl, 1 mM KCl, 2.4 mM $NaHCO_3$, 0.82 mM $MgSO_4$, 10 mM HEPES, pH 7.5).

Subsequently oocytes were homogenized in 1.5 ml of buffer HbA (20 mM Tris, 5 mM $MgCl_2$, 5 mM NaH_2PO_4, 1 mM EDTA, 80 mM sucrose, pH 7.4) containing protease inhibitor (Complete; Roche Applied Science) and centrifuged for 30 s at 10 × *g* at 4 °C after which 1.3 ml of the sample supernatant was removed (to be saved for subsequent preparation of total membranes; see below), and 1 ml of HbA was added to the silica beads. This centrifugation and exchange of HbA was repeated three times, but centrifugation changed from twice at 10 × *g* to once at 20 × *g* to once at 40 × *g*. After the last centrifugation step, HbA was removed, and plasma membranes were spun down for 30 min at 16,000 × *g* at 4 °C and resuspended in Laemmli buffer (37) (4 μl/oocyte).

Preparation of Total Membranes from X. laevis Oocytes—To remove yolk platelets, the supernatant from homogenized oocytes in HbA containing protease inhibitor (see above) was centrifuged once for 3 min at 2,000 × *g* at 4 °C, and the pellet was discarded. Total membranes in the supernatant were spun down for 30 min at 16,000 × *g* at 4 °C and resuspended in 4 μl/oocyte Laemmli buffer (37).

Immunoblotting—Protein samples equivalent to two oocytes were separated on 10% SDS-polyacrylamide gels and blotted on nitrocellulose membranes (Roth). The α- and β-subunits of the rat gastric H,K-ATPase were detected with the polyclonal anti-H,Kα-antibody HK12.18 (5) (Merck) and the monoclonal anti-H,Kβ-antibody 2G11 (23) (Acris Antibodies), respectively.

Subsequently blots were incubated with appropriate horseradish peroxidase-conjugated secondary antibodies (Dako), and proteins were visualized by using an enhanced chemiluminescence kit (Roche Applied Science).

Rb^+ Uptake Assay Using Atomic Absorption Spectrometry—Two days after injection, noninjected control oocytes and H,K-ATPase-expressing oocytes were preincubated for 15 min in a Rb^+- and K^+-free solution (90 mM TMACl or NaCl, 20 mM tetraethylammonium chloride, 5 mM $BaCl_2$, 5 mM $NiCl_2$, 10 mM HEPES, pH 7.4) containing 100 μM ouabain to ensure inhibition of the endogenous Na,K-ATPase and then incubated for 15 min under temperature control in Rb^+ flux buffer at 21 °C (5 mM RbCl, 85 mM TMACl or NaCl, 20 mM tetraethylammonium chloride, 5 mM $BaCl_2$, 5 mM $NiCl_2$, 10 mM MES, pH 5.5, 100 μM ouabain). After three washing steps in Rb^+-free washing buffer (90 mM TMACl or NaCl, 20 mM tetraethylammonium chloride, 5 mM $BaCl_2$, 5 mM $NiCl_2$, 10 mM MES, pH 5.5) and one wash in water, each individual oocyte was homogenized in 1 ml of Milli-Q® water (Millipore, Billerica, MA).

To determine the apparent constant $K_{½}$ for half-maximal activation of the H,K-ATPase by rubidium, the sum of [TMACl or NaCl] plus [RbCl] in the Rb^+ flux buffer was kept constant at 90 mM, *e.g.* 1 mM RbCl + 89 mM TMACl (or NaCl). After subtraction of the mean of Rb^+ uptake into control oocytes of the same batch at a given RbCl concentration, the data were fitted to a Michaelis-Menten type function.

$$v = v_{max} \cdot \frac{[S]}{K_{0.5} + [S]} \quad \text{(Eq. 1)}$$

Oocyte homogenates were analyzed by atomic absorption spectroscopy using an AAnalyst800™ spectrometer (Perkin Elmer Life Sciences). From oocyte homogenates (typically 1 ml) samples of 20 μl were automatically transferred into a transversely heated graphite furnace and subjected to a temperature protocol according to the manufacturer's procedures (conditions are available on request), and absorption was measured at 780 nm using a rubidium hollow cathode lamp (Photron, Melbourne, Australia). After Zeeman background correction, Rb^+ contents were calculated by comparison with standard calibration curves (measured between 0 and 50 μg/liter Rb^+). The detection limit (characteristic mass) of Rb^+ is ~10 pg.

Oocyte Pretreatment, Fluorescence Labeling, and Experimental Solutions—Prior to functional studies on Na,K-ATPase-expressing oocytes, cells were first incubated for 45 min in Na^+ loading buffer (110 mM NaCl, 2.5 mM sodium citrate, 5 mM MOPS, 5 mM Tris, pH 7.4), and then for 15 min in postloading buffer (100 mM NaCl, 1 mM $CaCl_2$, 5 mM $BaCl_2$, 5 mM $NiCl_2$, 5 mM MOPS/Tris, pH 7.4 (38)) to elevate the intracellular Na^+ concentration. For voltage clamp fluorometry, site-specific labeling was achieved by incubating oocytes in postloading buffer containing 5 μM TMRM (Molecular Probes; stock solution, 5 mM in DMSO) for 5 min at room temperature in the dark followed by extensive washes in dye-free postloading buffer. Measurements under high extracellular Na^+/K^+-free conditions were carried out in Na^+ test solution (100 mM NaCl, 5 mM $BaCl_2$, 5 mM $NiCl_2$, 5 mM MOPS/Tris, pH 7.4, 10 μM ouabain). The following solution was used for VCF measurements on H,K-ATPase: 90 mM TMACl or NaCl, 20 mM tetraethylammonium chloride, 5 mM $BaCl_2$, 5 mM $NiCl_2$, 10 mM MES, pH 5.5. Stationary currents of the Na,K-ATPase were measured upon a solution exchange from 0 to 10 mM K^+ (10 mM KCl, 90 mM NaCl, 5 mM $BaCl_2$, 5 mM $NiCl_2$, 5 mM MOPS/Tris, pH 7.4, 10 μM ouabain). To determine the apparent constant $K_{½}$ for half-maximal activation of the Na,K-ATPase by K^+, the sum of [NaCl] plus [KCl] in the Na^+ test solution was kept constant at 100 mM, *e.g.* 1 mM KCl + 99 mM NaCl. After rundown correction of stationary currents (if necessary) at a given K^+ concentration, the data were fitted to a Michaelis-Menten type function (Equation 1). The sheep Na,K-ATPase could be inhibited by 10 mM ouabain, and the rat gastric H,K-ATPase could be inhibited by 10 μM SCH28080 (Sigma-Aldrich) or 30 μM omeprazole (Biotrend, Zürich, Switzerland).

Voltage Clamp Fluorometry—An oocyte perfusion chamber was mounted in an Axioskop 2FS epifluorescence microscope (Carl Zeiss, Göttingen, Germany) equipped with a 40× water immersion objective (numerical aperture = 0.8). Currents were measured using a two-electrode voltage clamp amplifier (Turbotec 05, npi electronic GmbH, Tamm, Germany). Fluorescence was excited with a 100-watt tungsten lamp using filters 535DF50 (excitation), 565EFLP (emission), and 570DRLP (dichroic; all from Omega Optical, Brattleboro, VT). Fluorescence was measured with a PIN-022A photodiode (United Detector Technologies, Hawthorne, CA) mounted to the microscope camera port. Photocurrents were amplified by a low noise current amplifier (DLPCA-200, FEMTO, Berlin, Germany). Fluorescence and currents were recorded simultaneously using a Digidata 1322A interface and subsequently analyzed with Clampex 9.2 and Clampfit 9.2 software (Molecular Devices, Sunnyvale, CA). Apparent $K_{½}$ values for extracellular K^+ were obtained by titration experiments as described previously (28).

Analysis of Transient Currents of the Na,K-ATPase—Pre-steady-state currents under high extracellular Na^+/K^+-free conditions were obtained by subtracting the current responses to voltage steps from −40 mV to values between +60 and −180 mV (20-mV increments) in the presence of 10 mM ouabain (inhibiting the endogenously as well as the heterologously expressed pump) from currents measured in the presence of 10 μM ouabain (inhibiting only the endogenous Na,K-ATPase). The resulting difference currents were fitted monoexponentially, disregarding the first 3–5 ms after the voltage step to exclude capacitive artifacts. The translocated charge Q was calculated from the integral of the fitted transient currents, and the resulting Q-V curves were approximated by a Boltzmann-type function,

$$Q(V) = Q_{max} + \frac{Q_{max} - Q_{min}}{\left(1 + \exp\left(\frac{z_q \cdot F}{R \cdot T}(V - V_{0.5})\right)\right)} \quad \text{(Eq. 2)}$$

where Q_{min} and Q_{max} are the saturating values of translocated charge, $V_{0.5}$ is the midpoint potential, z_q is the fraction of charge displaced through the entire transmembrane field, F is the Faraday constant, R is the molar gas constant, T is the temperature (in K), and V is the transmembrane potential. All experiments were performed at 22–24 °C.

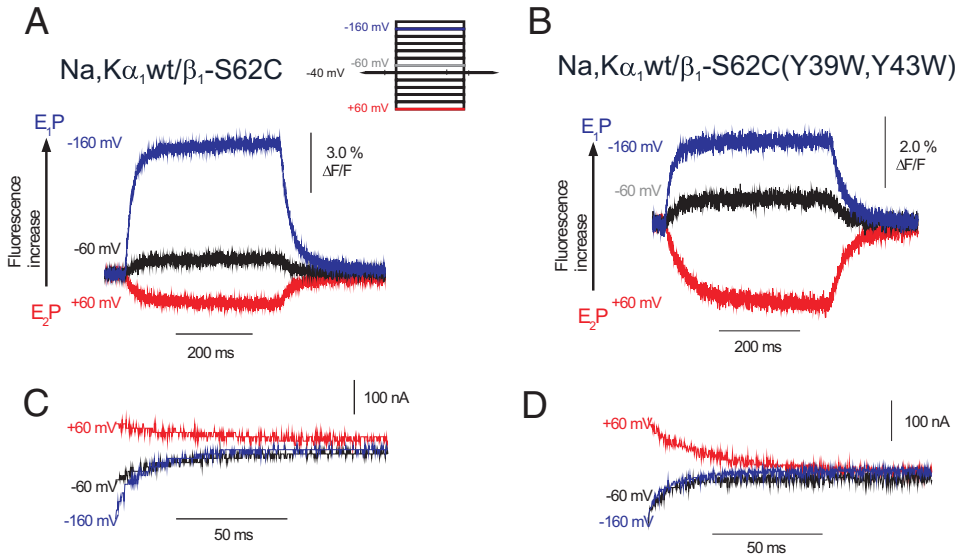

FIGURE 2. **Voltage pulse-induced fluorescence changes and transient currents of site-specifically labeled Na,K-ATPase wild type and β_1-(Y39W,Y43W) mutant enzymes.** Fluorescence amplitudes (*A* and *B*) and transient currents (*C* and *D*) in response to voltage pulses from −40 mV to three representative voltages (+60, −60, and −160 mV; see *inset*) under extracellularly high Na^+, K^+-free conditions are shown. Data originated from individual oocytes co-expressing the wild type Na,K-ATPase α_1-subunit with either the unmodified reporter construct β_1-S62C (*A* and *C*) or the reporter construct β_1-S62C(Y39W,Y43W) carrying tryptophan replacements of the two conserved tyrosines (*B* and *D*).

Extracellular pH Measurements—A qualitative assay for the acidification of the extracellular medium mediated by H^+ secretion of *Xenopus* oocytes expressing gastric H,K-ATPase was carried out according to Jaisser *et al.* (39). Two days after injection, oocytes were incubated for 5 min in a weakly buffered solution (70 mM TMACl, 20 mM RbCl, 5 mM $BaCl_2$, 5 mM $NiCl_2$, 500 μM MOPS, adjusted to pH 7.4 with tetramethylammonium hydroxide) containing the pH indicator phenol red (200 μg/ml). In some experiments, SCH28080 (100 μM) was added to the solution. Oocytes were placed individually in a small drop (0.5–1 μl) of the same solution under mineral oil. Every 2 min a color picture was taken at room temperature.

RESULTS AND DISCUSSION

E_1P/E_2P Conformational Distribution and Kinetics of the E_1P/E_2P Transition for Na,K-ATPase Wild Type and β-(Y39W,Y43W) Mutant Enzymes—To determine whether the double mutation Y39W/Y43W in the Na,K-ATPase β_1-subunit causes the proposed shift of the conformational equilibrium of the enzyme toward E_1 (25), the two tryptophans were introduced into the reporter construct β_1-S62C and co-expressed with the α_1-subunit in *Xenopus* oocytes. Upon labeling with the environmentally sensitive dye TMRM, we applied voltage jumps under extracellularly high Na^+, K^+-free conditions. Under these conditions, the sodium pump carries out Na^+/Na^+ exchange where the enzyme shuttles exclusively between E_1P/E_2P states of the catalytic cycle. The ratio E_1P/E_2P is increased by extracellular Na^+, but the effect is opposed if extracellular K^+ is also present (40, 41). Fig. 2 shows fluorescence signals and transient currents in response to three representative voltage steps (−160, −60, and +60 mV) for an oocyte expressing the Na,K-ATPase α_1-subunit together with either the reference construct β_1-S62 (*A* and *C*, respectively) or the mutated β_1-subunit variant β_1-S62C(Y39W,Y43W) (*B* and *D*, respectively).

Of note, voltage jumps to extremely hyperpolarizing potentials (−160 mV), which force the sodium pump into the E_1P state, result in a relative fluorescence increase (as described in Refs. 28 and 29), which is more pronounced for the wild type (Fig. 2*A*) than for the mutant enzyme (Fig. 2*B*). In contrast, E_2-promoting positive membrane potentials lead to a relative fluorescence decrease, which is substantially larger for the double Trp mutant than for the non-mutated construct. This indicates that *e.g.* at −40 mV the dynamic equilibrium between the two principal conformations is shifted toward E_1 for the β-variant enzyme. This shift of the voltage-dependent distribution is also reflected by the concomitantly recorded transient currents of the mutant that exhibit larger amplitudes for voltage jumps to positive potentials (*e.g.* +60 mV; Fig. 2*D*) compared with the corresponding wild type signals (Fig. 2*C*).

Both the resulting voltage-dependent distribution of transported charge (Q-V curve; Fig. 3*A*) and the $(1 - \Delta F/F)$-V distribution (Fig. 3*B*) can be fitted to a Boltzmann function, yielding midpoint potentials that are significantly more positive for the β_1-S62C (Y39W,Y43W) mutant than for the β_1-S62C reference enzyme (see Table 1). Moreover the voltage-dependent reciprocal time constants (τ^{-1}) of transient currents (Fig. 3*C*) and of fluorescence changes (Fig. 3*D*) are also shifted by almost +50 mV toward depolarizing potentials for the variant sodium pumps. Notably the reciprocal time constants are significantly larger for the mutant enzyme at negative potentials but not at positive potentials. This indicates that only the apparent rate constant for reverse binding of extracellular Na^+ and the subsequent conformational change from E_2P to E_1P is increased for the mutant. This is in agreement with the increased apparent affinity for extracellular Na^+ as reported by Hasler *et al.* (25) that was most pronounced at hyperpolarizing potentials (as inferred from the sodium-dependent inhibition of pump currents especially at hyperpolarizing membrane potentials). The increased apparent rate constant for the backward reaction sequence (extracellular Na^+ reverse binding/E_2P/E_1P transition) observed for the mutant in the current study can also account for the increased apparent $K_{½}$ of the mutant for extracellular K^+ that was shown to be more pronounced at high extracellular Na^+ concentrations (25). With increasing extracellular K^+ concentrations a relative decrease of the fluorescence amplitudes $\Delta F/F$ of TMRM-labeled Na,K-ATPase is observed (Fig. 4, *A*–*E*). Thus, the apparent $K_{½}$ for extracellular K^+ can be determined from the K^+ dependence of this decrease as demonstrated previously (28). Using this independent

approach, we confirm here the reduced extracellular K^+ affinity for the mutant in presence of Na^+ (Fig. 4*F*).

Molecular Determinants for the E_2-stabilizing Effect Mediated by the Two Conserved Tyrosines—To further clarify which particular property of the β-TMD tyrosines is necessary to maintain the observed E_2 preference in the E_1P/E_2P distribution within the reference construct β_1-S62C, we determined the E_1P/E_2P conformational distribution of additional β_1-S62C variants: β_1-S62C(Y39S,Y43S) was chosen to conserve the hydroxyl group, and β_1-S62C(Y39F,Y43F) was chosen to maintain the phenyl moiety of the side chains. According to the Boltzmann parameters obtained for the $(1 - \Delta F/F)$-V curves of these two mutants (Table 1), a significant shift of the conformational equilibrium toward the E_1 state is observed for both, but the effect is more pronounced for the serine replacements. This indicates that both the hydroxyl group and the aromatic phenyl moiety may be involved in the interaction, but surprisingly the aromatic ring appears to be more important. Apparently not only "classical" H-bonds (illustrated in Fig. 1, *A* and *B*) are responsible for the E_2-stabilizing effect of the two tyrosines but possibly also amino-aromatic interactions (or amino-aromatic H-bonds) with side chain or even backbone amides in the α-TMD7 (see below). Notably according to Hasler *et al.* (25), a significantly reduced apparent K^+ affinity was only observed for β-(Y39S,Y43S) but not for β-(Y39F,Y43F), corroborating this interpretation. Our results also demonstrate that the fluorometric technique applied here is a substantially more sensitive method. It is able to detect even subtle changes in the E_1P/E_2P poise, which may have no direct consequences on the apparent ion affinities but still are relevant to identify the molecular determinants for the interaction patterns of the tyrosine side chains.

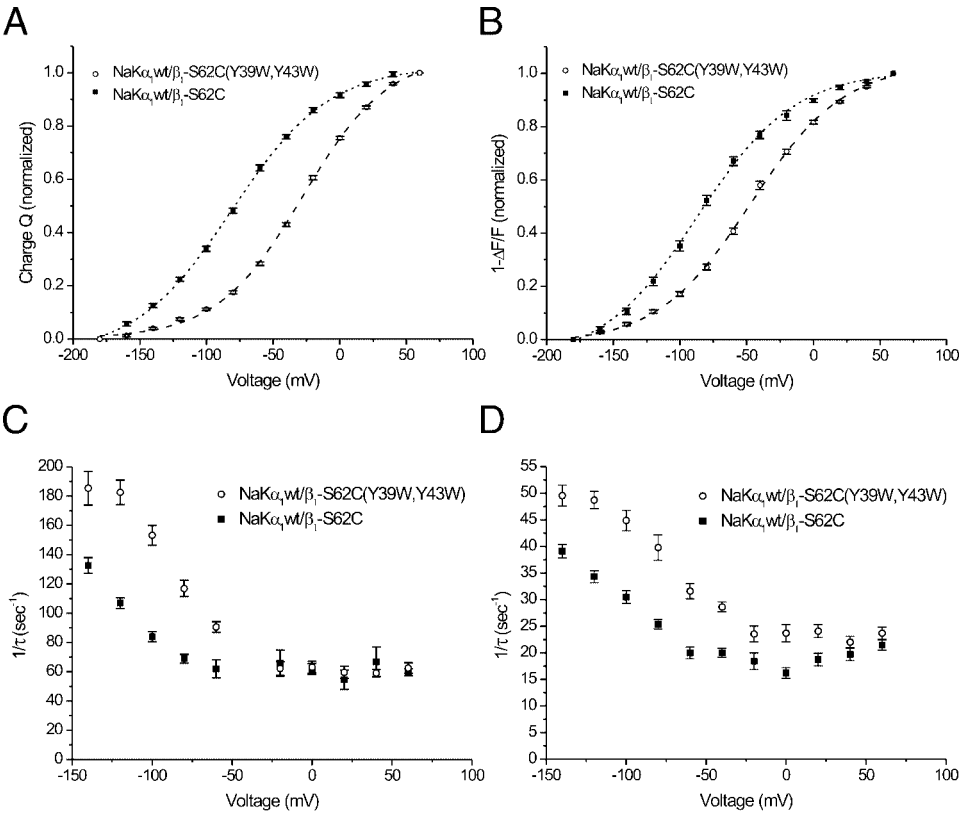

FIGURE 3. **Voltage dependence of the E_1P/E_2P distribution and kinetics of the E_1P/E_2P transition for Na,K-ATPase wild type and β_1-(Y39W,Y43W) variant enzymes.** *A* and *B*, voltage-dependent distributions of transported charge *Q* (*A*) and of fluorescence amplitudes $1 - \Delta F/F$ (*B*) for Na,K-ATPase consisting of the wild type α_1-subunit and either unmodified reporter construct β_1-S62C (■) or mutated β_1-S62C(Y39W,Y43W) (○). Data are means ± S.E. of 20–25 oocytes from three to four different oocyte batches normalized to saturating values at −180 mV after subtracting the values for +60 mV. A curve corresponding to the fit of a Boltzmann function is superimposed (*dashed lines*; see Table 1 for fit parameters). *C* and *D*, reciprocal time constants of voltage jump-induced transient currents (*C*) and fluorescence changes (*D*) for oocytes expressing the Na,K-ATPase wild type α_1-subunit together with either β_1-S62C (■) or β_1-S62C(Y39W,Y43W) (○). Data are means ± S.E. of 10–15 (*C*) or 20–25 (*D*) oocytes from three to four different oocyte batches.

E_1P/E_2P Conformational Distribution, Apparent Rb^+ Affinities, and SCH28080 Sensitivity of the H,K-ATPase Wild Type and β-(Y44W,Y48W) Variant Enzymes—The study by Hasler *et al.* (25) also included a chimeric β-subunit consisting of the cytoplasmic and transmembrane domains of the Na,K β_1-subunit and the ectodomain of the gastric H,K-ATPase β-subunit that was co-expressed with the Na,K-ATPase α-subunit. Because the tryptophan mutations were accordingly introduced into a TMD derived from the Na,K-ATPase β_1-subunit and its effects were

TABLE 1

Parameters from fits of a Boltzmann function to Q-V distributions of Na,K-ATPase and (1 − ΔF/F)-V distributions of Na,K-ATPase or H,K-ATPase β-variants

	Boltzmann parameter $(1 - \Delta F/F)$-V curves		Boltzmann parameter Q-V curves	
	$V_{0.5}$	z_q	$V_{0.5}$	z_q
	mV		*mV*	
NaKα$_1$wt/β$_1$-S62C	−94.8 ± 4.8	0.74 ± 0.01	−76.6 ± 4.8	0.77 ± 0.03
NaKα$_1$wt/β$_1$-S62C(Y39W,Y43W)	−44.8 ± 1.5	0.73 ± 0.03	−29.3 ± 0.9	0.79 ± 0.03
NaKα$_1$wt/β$_1$-S62C(Y39F,Y43F)	−79.1 ± 3.6	0.72 ± 0.02	ND[a]	ND
NaKα$_1$wt/β$_1$-S62C(Y39S,Y43S)	−56.1 ± 8.0	0.74 ± 0.03	ND	ND
HKα-S806C/βwt[b]	−125.1 ± 11.4	0.49 ± 0.07		
HKα-S806C/β-(Y44W,Y48W)[b]	−90.0 ± 3.4	0.68 ± 0.06		

[a] ND, not determined.
[b] Determined in 90 mM TMACl, pH 5.5.

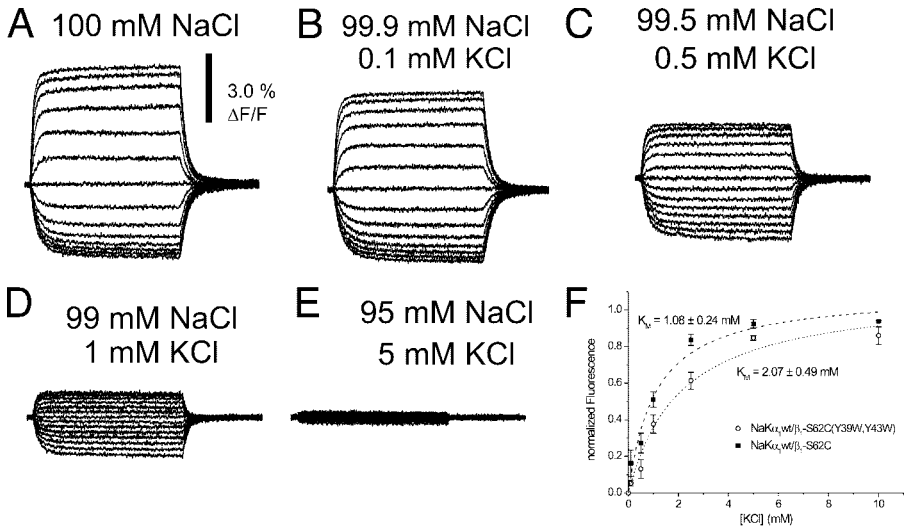

FIGURE 4. **Determination of the apparent $K_{1/2}$ for extracellular K^+ of Na,K-ATPase $\alpha_1$wt/β_1-S62C and $\alpha_1$wt/β_1-S62C(Y39W,Y43W) variant enzymes by fluorescence titration experiments.** Shown is a representative fluorescence titration experiment of a single oocyte expressing $\alpha_1$wt/β_1-S62C. Voltage jumps were applied from a holding potential of −40 mV to potentials between +60 and −180 mV at different external K^+ concentrations (0, 0.1, 0.5, 1, and 5 mM KCl; *A–E*) in presence of Na^+. *F*, K^+ activation curves resulting from titration experiments (see Ref. 28 for details) on $\alpha_1$wt/β_1-S62C (■) and $\alpha_1$wt/β_1-S62C(Y39W,Y43W) (○) Na,K-ATPase-expressing oocytes. Data are means ± S.E. of three to five independent experiments. The shown apparent $K_{1/2}$ values (1.08 ± 0.24 mM for $\alpha_1$wt/β_1-S62C and 2.07 ± 0.49 mM for $\alpha_1$wt/β_1-S62C(Y39W,Y43W)) were obtained from a fit (*dashed lines*) of a Michaelis-Menten-type function to the data.

monitored by Na,K-ATPase transport activity, this chimeric ATPase does not represent an optimal system to clarify the functional relevance of the conserved tyrosines for H,K-ATPase ion transport activity. We therefore extended the current study to the true oligomeric form of the gastric H,K-ATPase by co-expressing the H,K-ATPase β-subunit with an α-subunit variant carrying a single cysteine replacement (S806C) in the M5/M6 loop that is necessary to enable voltage clamp fluorometry but does not impair enzyme activity (29, 30). Fig. 5*A* shows the voltage dependence of fluorescence changes obtained for oocytes co-expressing the H,K-ATPase α-S806C variant together with either the wild type H,K β-subunit or a H,K-ATPase β-subunit carrying the Y44W,Y48W mutation. In analogy to Na,K-ATPase, the voltage dependence of fluorescence amplitudes observed for the H,K-ATPase β-(Y44W,Y48W) is shifted toward depolarizing potentials compared with proteins comprising wild type β-subunits. The resultant Boltzmann distribution is characterized by a substantially smaller slope, z_q, than the corresponding Na,K-ATPase curves (see Tables 1 and 2), thus indicating a reduced voltage sensitivity as described previously (30). This can be interpreted as a reduced dielectric depth of a so-called "ion access channel" that intracellular protons (or hydronium ions) pass upon voltage pulses to reach or exit from the cation binding sites. Because a smaller fraction of the transmembrane potential is accordingly sensed by the transported charge, the process is less electrogenic than the extracellular Na^+ binding/release, indicating a deeper ion well in the case of the sodium pump (42).

Because saturation of fluorescence amplitudes cannot be reached in the experimentally accessible voltage range, the saturating values of the Boltzmann curves had to be determined by extrapolation of the fit function. Of note, only small fluorescence changes ($\Delta F/F \sim 0.5$–2%) were consistently observed for the β-(Y44W,Y48W) variant, corresponding to about 10% of the wild type fluorescence signals ($\Delta F/F \sim$ 5–20%). To account for this, the saturation level used for normalization of the mutant has been arbitrarily set to 0.1 (instead of 1 for the wild type), which is illustrated by the different scaling of the *y axis* on the *right* in Fig. 5*A*.

To determine whether the conformational shift toward E_1 observed here for the H,K-ATPase β-(Y44W,Y48W) mutant also causes changes in cation affinities, we determined the apparent Rb^+ affinity in Rb^+ uptake experiments. As illustrated in Fig. 5*B*, the apparent affinity of the variant enzyme for extracellular Rb^+ in the absence of extracellular Na^+ is drastically reduced by a factor of more than 20. If the apparent $K_{1/2}$ is determined in the presence of extracellular Na^+ (Fig. 5*C*), the apparent $K_{1/2}$ values are substantially larger for both the wild type and the β-(Y44W,Y48W) variant enzyme, but the affinity decrease caused by the double Trp mutation is still observed, albeit it is less pronounced. Interestingly the apparent $K_{1/2}$ of the wild type H,K-ATPase is more strongly influenced by the presence of Na^+ because it is almost 7-fold higher than in absence of Na^+, whereas the apparent $K_{1/2}$ of the mutant is increased by a factor of less than 1.5. Considering the E_1 shift observed for the mutant enzyme in the current study, the observation has a reasonable explanation: the effects of sodium ions on the H,K-ATPase have been described in various studies (43–46), and it was shown that they compete with K^+ binding to the extracellular binding sites (46). Therefore the wild type enzyme, which is predominantly in the E_2 state, is more susceptible to this competition of Na^+ ions, which in effect reduces the apparent Rb^+ affinity in the presence of Na^+. In contrast, the β-(Y44W,Y48W) variant enzyme is preferably present in the E_1 state and thus cannot efficiently bind extracellular Rb^+. Accordingly this mutant exhibits a substantially reduced apparent Rb^+ affinity irrespective of the presence of Na^+ ions, which exert their competitive effect only in the E_2 state. Fig. 5*E* illustrates another interesting property of the H,K-ATPase β-(Y44W,Y48W) mutant: it exhibits a strongly reduced sensitivity toward the inhibitor SCH28080. Whereas for the wild type enzyme Rb^+ uptake is readily inhibited by the compound already at concentrations as low as 10 μM (to about 10–15% residual activity at saturating 5 mM RbCl; see Fig. 5*D*), the variant is only partially inhibited to residual activities of 30–80% depending on the extracellular Rb^+ concentration even at higher SCH28080 concentrations up to 150 μM (Fig. 5*E*). Because SCH28080 is known to be an E_2-specific inhibitor (47), the observed insensitivity of the variant enzyme again reflects its preference for the E_1 state, which is in close analogy to the

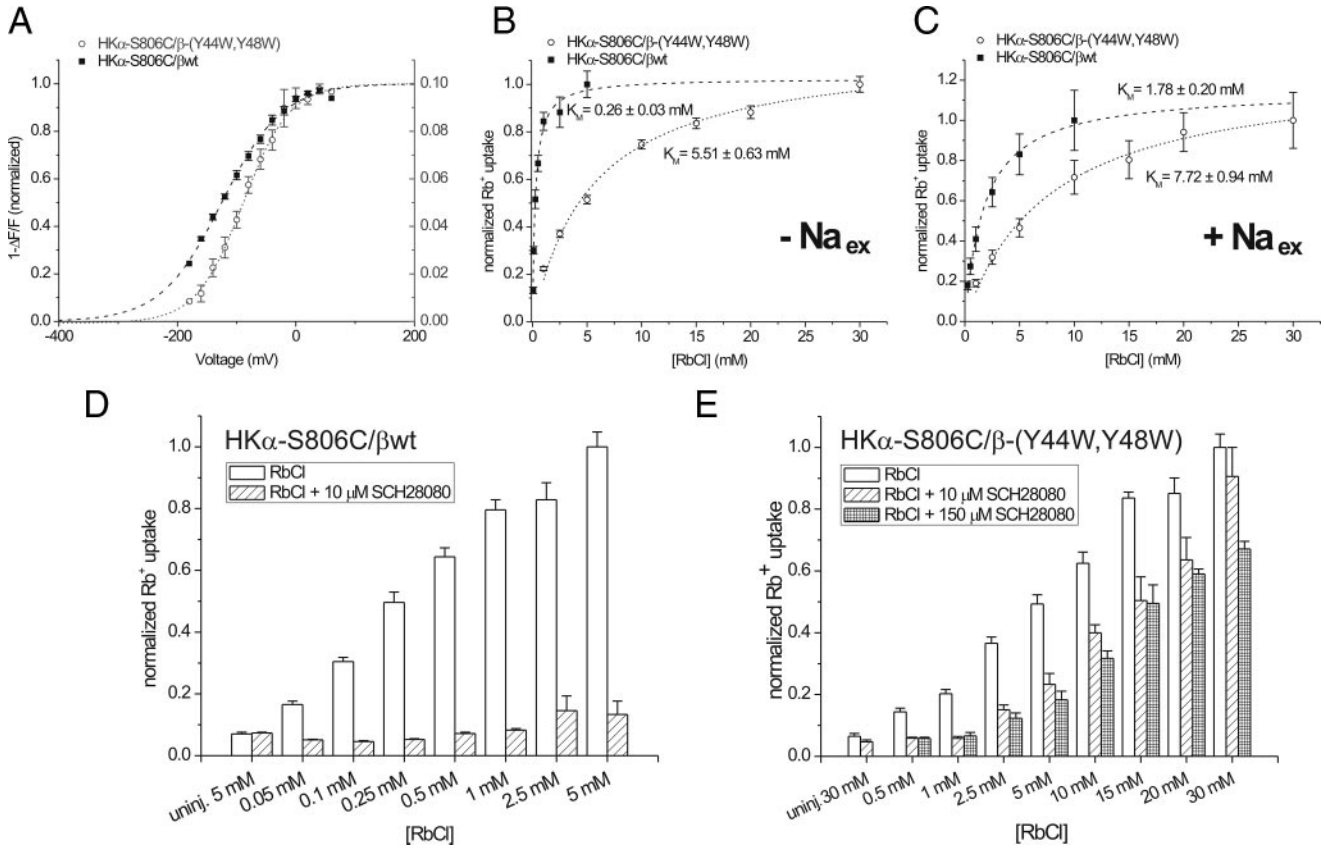

FIGURE 5. **Functional properties of the gastric H,K-ATPase β-(Y44W,Y48W) mutant enzyme.** *A*, voltage-dependent E_1P/E_2P distribution of fluorescently labeled αS806C/βwt (■) and αS806C/β-(Y44W,Y48W) (○) H,K-ATPase enzymes resulting from fluorescence responses upon voltage jumps from a holding potential of −40 mV to values between +60 and −180 mV (20-mV increments) at pH 5.5. Data are means ± S.E. of 10–15 oocytes from two to three different oocyte batches. A curve resulting from a fit of a Boltzmann function is superimposed (see Table 1 for parameters). Fluorescence amplitudes $1 - \Delta F/F$ were normalized to saturation values from the fits. To account for the substantial differences in the fluorescence amplitudes, the saturation values were set to 1 for the wild type and to 0.1 for the β-(Y44W,Y48W) mutant. *B* and *C*, Michaelis-Menten plots for concentration-dependent Rb^+ uptake by H,K-ATPase in the absence (*B*) or presence (*C*) of extracellular Na^+ at pH 5.5. Oocytes were injected with αS806C mutant and the wild type (■) or the (Y44W,Y48W) variant (○) β-construct cRNA, respectively. Data were normalized to Rb^+ uptake at saturating RbCl concentrations corresponding to values between 20 and 30 pmol min^{-1}/oocyte for different oocyte batches (αS806C/βwt: 29.3, 27.4, and 30.8 in the absence of Na^+; 21.1 and 23.4 in the presence of Na^+; αS806C/β-(Y44W,Y48W): 28.4 and 33.9 in the absence of Na^+; 32.6 and 30.1 in the presence of Na^+). Data are means ± S.E., $n = 8–12$ oocytes from two or three independent experiments. Apparent half-maximal activation constants, $K_{1/2}$ (in mM), were obtained from a fit of a Michaelis-Menten type function to the data (*dashed lines*). *D* and *E*, SCH28080 sensitivity of Rb^+ uptake by oocytes expressing HKα-S806C/βwt (*D*) or HKαS806C/β-(Y44W,Y48W) (*E*) H,K-ATPase complexes. Rb^+ uptake was determined at pH 5.5 in extracellular Na^+-free solutions containing different Rb^+ concentrations in the absence (*white bars*) or presence of SCH28080 (*hatched bars*, 10 μM; *crossed bars*, 150 μM). Data were normalized to Rb^+ uptake at saturating RbCl concentrations. Data are means ± S.E., $n = 10–15$ oocytes from at least two independent sets of experiment. *uninj.*, uninjected.

TABLE 2

Parameters from fits of a Boltzmann function to (1 − ΔF/F)-V or Q-V distributions of Na,K-ATPase or H,K-ATPase α-variants

	Boltzmann parameter (1 − Δ *F*/*F*)-*V* curves		Boltzmann parameter *Q*-*V* curves	
	$V_{0.5}$	z_q	$V_{0.5}$	z_q
	mV		*mV*	
NaKα$_1$wt/β$_1$-S62C	−94.8 ± 4.8	0.74 ± 0.01	−76.6 ± 4.8	0.77 ± 0.03
NaKα$_1$-Y847W/β$_1$-S62C	−102.4 ± 5.7	0.56 ± 0.04	−82.8 ± 3.2	0.56 ± 0.03
NaKα$_1$-G848W/β$_1$-S62C	−66.0 ± 2.1	0.70 ± 0.02	−44.8 ± 1.2	0.76 ± 0.01
NaKα$_1$-G848F/β$_1$-S62C	−67.9 ± 4.7	0.74 ± 0.01	−45.9 ± 4.1	0.76 ± 0.02
NaKα$_1$-Q849W/β$_1$-S62C	−71.6 ± 2.6	0.75 ± 0.05	−50.6 ± 2.8	0.76 ± 0.03
NaKα$_1$-Q849G/β$_1$-S62C	−99.7 ± 4.7	0.72 ± 0.02	−86.3 ± 3.6	0.66 ± 0.02
NaKα$_1$-Q849H/β$_1$-S62C	−93.8 ± 3.2	0.72 ± 0.01	−77.4 ± 2.5	0.75 ± 0.01
HKα-S806C/β wt	−110.8 ± 8.6	0.34 ± 0.01		
HKα-S806C(Y863W)/β wt	+74.3 ± 12.7	0.32 ± 0.02		
HKα-S806C(F864W)/β wt	−58.0 ± 7.0	0.28 ± 0.02		
HKα-S806C(Q865W)/β wt	−67.9 ± 3.6	0.36 ± 0.01		

reduced vanadate sensitivity of the homologous Na,K-ATPase mutation β-(Y39W,Y43W) described by Hasler *et al.* (25). Control experiments showed, however, that Rb^+ uptake by the variant H,K-ATPase is inhibited to an extent similar to that of uptake of the wild type enzyme by omeprazole (data not shown). Because this inhibitor binds covalently to the H,K-pump (48), steady-state inhibition caused by the compound is not conformation-specific.

H^+ Secretion of H,K-ATPase Wild Type and β-(Y44W,Y48W) Variant Enzymes—The data presented here suggest a common E_2-stabilizing effect of the two conserved β-subunit tyrosines in both Na,K- and H,K-ATPase that is apparently disrupted by the tryptophan replacement in the β-variants. Therefore, as argued for the accelerated apparent rate constant for reverse binding of extracellular Na^+ and the subsequent E_2P/E_1P conformational shift for the β_1-(Y39W,Y43W) Na,K-ATPase variant, in the case of the H,K-ATPase containing a double Trp-mutated β-subunit the observed E_1 shift should have a similar effect on extracellular H^+ reverse binding/E_2P/E_1P conversion. This in fact would kinetically interfere with luminal H^+ release from the external binding sites. To test this hypothesis, we performed a simple assay to evaluate extracellular acidification of wild type or mutant H,K-ATPase-expressing oocytes. Whereas in wild type H,K-ATPase-expressing oocytes the extracellular medium is substantially acidified (to at least pH 4) within 40 min as indicated by the distinct change in phenol red color (Fig. 6, *A* and *B*, *upper* two oocytes), no pH change is observed for oocytes expressing the β-(Y44W,Y48W) mutation (Fig. 6, *A* and *B*, *lower* two oocytes) even when monitored for longer time periods. Please note that the concentration of RbCl in the extracellular medium was as high as 20 mM, thus representing saturating conditions even for the Y44W/Y48W mutant, which has a substantially higher apparent $K_{½}$, however, without concomitant changes in v_{max} (see Fig. 5 legend). To demonstrate the specificity of the acidification, the assay was also carried out with uninjected oocytes and on wild type H,K-ATPase-expressing oocytes in the presence of 100 μM SCH28080 (Fig. 6*D*).

Fig. 7 summarizes the observed effects of the double tryptophan replacements on the conformational E_1P/E_2P distribution and cation affinities of Na,K-ATPase (Fig. 7, *A* and *B*) or H,K-ATPase (Fig. 7, *C* and *D*). In both enzymes, the mutations result in a shift of the conformational equilibrium toward E_1P as inferred from the voltage-dependent distribution of charge translocation and of fluorescence amplitudes (Fig. 3, *A* and *B*, for the sodium pump; Fig. 5*A* for the proton pump). Considering the voltage-dependent kinetics of charge translocation and fluorescence changes of the Na,K-ATPase β_1-(Y39W,Y43W) mutant compared with the wild type (Fig. 3, *C* and *D*), this can be assigned to an augmented apparent rate constant of Na^+ reverse binding (often designated as "backward" rate constant; k_{-1} in Fig. 7) because the differences in the reciprocal time constants are most pronounced at extremely negative potentials. At positive potentials, however, no significant changes are observed, which suggests that the "forward" rate constant (k_1 in Fig. 7) is unaltered by the mutation. Unfortunately because the voltage dependence of the apparent rate constants is shallow for the proton pump (30) and the fluorescence amplitudes for the H,K-ATPase β-(Y44W,Y48W) variant were quite small, it was not possible to demonstrate a similar phenomenon for the kinetics of the H,K-ATPase variant. Yet because the Na,K- and H,K-ATPase variants are mechanistically very similar (as summarized in Fig. 7), it is reasonable to assume that comparable k_1/k_{-1} alterations underlie the E_1 shift of the H,K-ATPase mutant. Moreover as the apparent v_{max} of Rb^+ uptake is unaffected for H,K-ATPase β-(Y44W,Y48W) (see Fig. 5 legend), it is likely that only the backward rate constant k_{-1} is changed

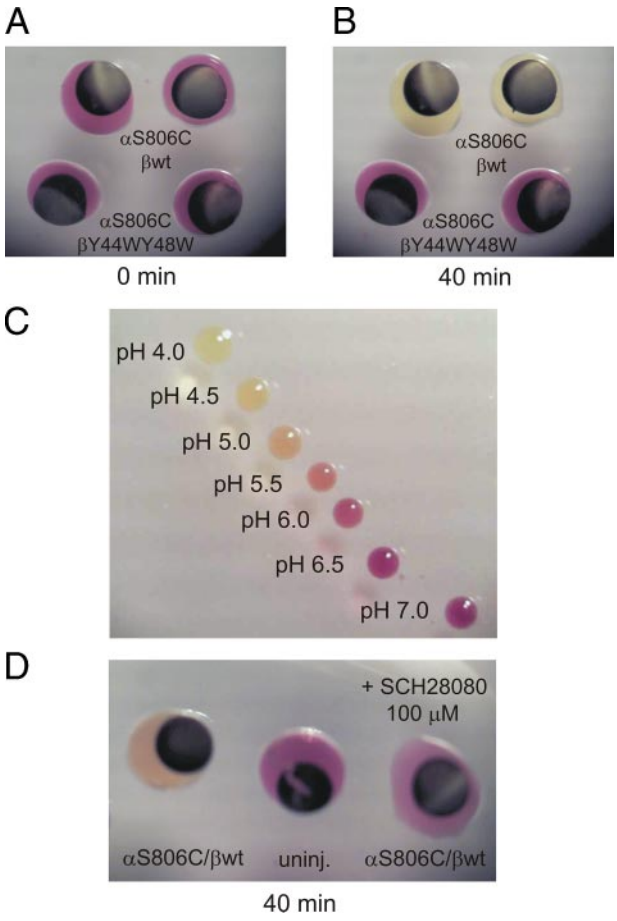

FIGURE 6. **Acidification assay for gastric H,K-ATPase-expressing oocytes.** *A*, oocytes co-expressing H,K-ATPase αS806C subunit with either βwt or β-(Y44W,Y48W) were placed under mineral oil in a droplet of weakly buffered solution at pH 7.4 containing pH indicator phenol red. *B*, after 40 min, a substantial acidification to at least pH 4 is observed for oocytes expressing αS806C/βwt H,K-ATPases (*B*, *upper* two oocytes) but not for those expressing the αS806C/β-(Y44W,Y48W) variant (*B*, *lower* two oocytes). One representative of several similar experiments is shown. *C*, extracellular solutions adjusted to different pH containing phenol red to provide a colorimetric scale. *D*, control experiments on uninjected (*uninj.*) or HKα-S806C/βwt-expressing oocytes in the presence of 100 μM SCH28080 after 40-min incubation.

because a decreased forward rate constant k_1 (which could as well explain an E_1 shift) would most likely also reduce the catalytic turnover number v_{max}. The shifted E_1P/E_2P distribution was shown to be accompanied by a decrease in the apparent affinity for extracellular K^+ of both enzymes, and enhanced rebinding of extracellular Na^+ for the sodium pump (or extracellular H^+ for the proton pump) was demonstrated for the variant pumps (Fig. 7, *B* and *D*). For the Na,K-ATPase, also an increased affinity for intracellular sodium was found (25). However, whether an increased proton affinity at the intracellular binding sites of H,K-ATPase is caused by the β-(Y44W,Y48W) mutation could not be determined by VCF experiments.

It should be emphasized that it is difficult to distinguish between cause and effect regarding the relation between shifts in conformational equilibria and changes in apparent cation affinities. If ion binding *per se* is disturbed, *e.g.* as a consequence of a mutation or reorientation of coordinating amino acids, this likely causes secondary shifts of the E_1P/E_2P distribution because of relative changes in k_1 or k_{-1}. However, regarding the

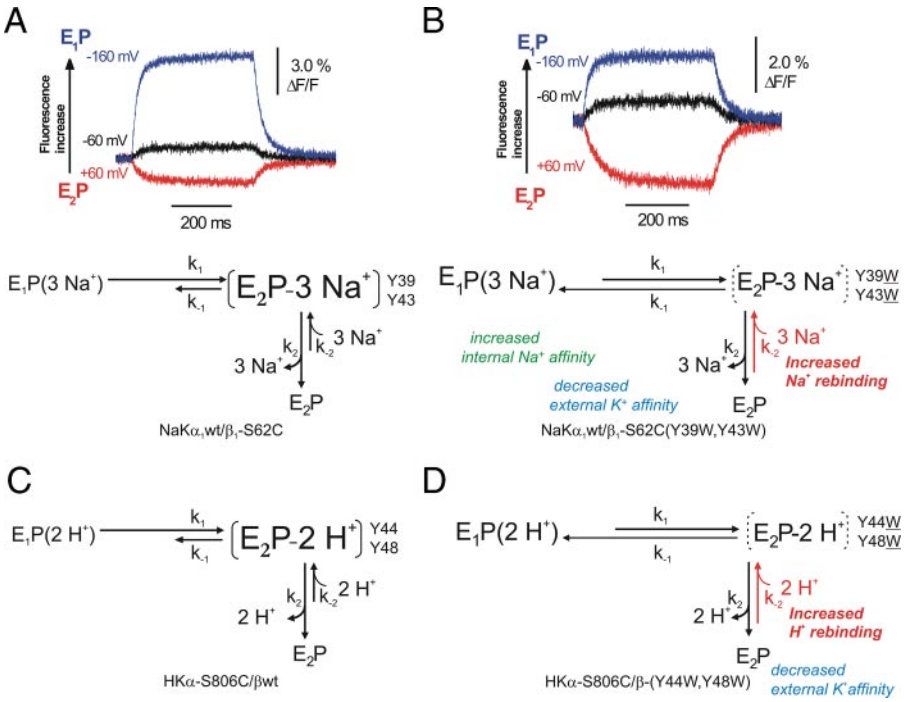

FIGURE 7. **Schematic illustration of the putative changes in the E_1P/E_2P conformational and external ion binding equilibria caused by the tryptophan replacements in the Na,K-ATPase (*A* and *B*) and H,K-ATPase (*C* and *D*) β-TMD.** According to this scheme the rate constants for the forward (k_1) and reverse (k_{-1}) E_1P/E_2P transitions are represented by *arrows*; k_2 and k_{-2} represent rate constants for extracellular release and reverse binding of Na^+ (*A* and *B*) or H^+ (*C* and *D*), respectively. Putative variations in these rate constants for the Na,K-ATPase β_1-S62C(Y39W,Y43W) mutant (*B*) or the H,K-ATPase β-(Y44W,Y48W) variant (*D*) from the "wild type" rate constants (*A* and *C*) are indicated by a *changed arrow length*. The hypothetical stabilization of the E_2 state by the two tyrosines is symbolized by *parentheses* (*A* and *C*), which are *dashed* for the mutant ATPases (*B* and *D*). For the Na,K-ATPase, representative fluorescence changes resulting from voltage-induced shifts of the E_1P/E_2P equilibrium are shown for the wild type (*A*) and the β_1-S62C(Y39W,Y43W) mutant (*B*) to demonstrate experimental support for the shifted E_1P/E_2P conformational distributions assumed here.

β-TMD mutants investigated here, we consider it more likely that the mutations introduced far from the site of cation coordination in the α-subunit have a destabilizing effect on the E_2 conformers of the holoenzyme. This in turn would result in a more effective ion binding to sites accessible in the E_1 state (intracellular Na^+) and a simultaneous decrease of ion binding to E_2-exposed sites (extracellular K^+ or Rb^+ but also their competitors Na^+ or H^+).

TMD7 Residues of Na,K- and H,K-ATPase α-Subunits Relevant for the E_2-stabilizing Interaction with the Two Conserved β-Tyrosines—According to the recently published crystal structure of the pig renal Na,K-ATPase in the Rb^+-occluded E_2 state (20), the two conserved β-tyrosines are at hydrogen bonding distance to TMD7 of the α-subunit (Fig. 1*B*). Interestingly TMD7 is partially unwound at this putative interaction site around Gly^{848}, resulting in a slight kink of the helix that in turn may permit the formation of a backbone hydrogen bond to the tyrosines of the β-subunit. Whereas in the H,K-ATPase sequence a phenylalanine (H,Kα-Phe^{864}) is located in homologous position to this glycine, the two adjacent residues Tyr^{847} and Gln^{849} on the Na,K-ATPase α-subunit are conserved (Fig. 1*D*); these residues correspond to residues H,Kα-Tyr^{863} and H,Kα-Gln^{865}, respectively. Apart from the backbone amide oxygen of Gly^{848}, the side chain of the conserved Gln^{849} is a likely candidate to form hydrogen bonds with the hydroxyl groups (or amino-aromatic interactions with the phenyl moiety) of the two tyrosines (Fig. 1*B*). Of note, these hydrogen bonds are unique for the whole α-β transmembrane interaction interface (Fig. 1*A*), thus underlining their potential contribution to the overall stabilization of the conformational state. If the distances and geometry of the interacting residues were slightly altered in the E_1 state, a conformational change toward E_1 would involve an energetically disfavorable breakage of some of these H-bonds. Accordingly a replacement of the two tyrosines by bulky tryptophans may disrupt this E_2-specific hydrogen bonding pattern and thus also the resulting E_2 stabilization, actually explaining the conformational shift toward the E_1 state observed for such mutant ATPases. If this is actually the case, tryptophan replacements of the potential interacting residues of the α-subunit should also impair this putative E_2 stabilization.

To test this hypothesis, we mutated the aforementioned three residues in the Na,K- and H,K-ATPase TMD7 and determined the voltage-dependent E_1P/E_2P distributions for these α-subunit mutants when co-expressed with Na,K-ATPase β_1-S62C or wild type H,K-ATPase β-subunits. The midpoint potentials of the resulting Q-V and $(1 - \Delta F/F)$-V curves for the Na,K-ATPase variants are shown in Fig. 8, *A* and *B*, respectively. Notably tryptophan replacements of Gly^{848} and Gln^{849} shifted the midpoint potentials of both $(1 - \Delta F/F)$-V and Q-V distributions substantially toward more positive potentials. Although the observed shifts were less pronounced than for the β_1-(Y39W,Y43W) mutant, still the idea is supported that Gly^{848} is involved in an E_2-stabilizing interaction with the β-subunit. To analyze the functional relevance of H,Kα-Phe^{864} found instead of Gly^{848} in the homologous position, we also investigated the Na,K-ATPase variant G848F. For this mutant, the voltage-dependent E_1P/E_2P distribution was similarly shifted toward E_1, thus indicating that the bulky phenylalanine side chain is as disruptive for the Na,K-ATPase α-β interaction as tryptophan. Both findings hint at an important role of the Gly^{848} backbone amide group for the interaction with the β-tyrosines that is apparently disrupted when larger side chains are introduced. Considering the Q849W mutant, a possible interpretation is that the observed E_1-shifted phenotype is directly caused by the removal of the glutamine side chain with its high propensity to participate in hydrogen bonding with β-Tyr^{39}. On the other hand, the properties of Q849W could merely be a consequence of the bulkiness of the introduced tryptophan side chain that interferes with the interaction mediated by the adjacent backbone amide

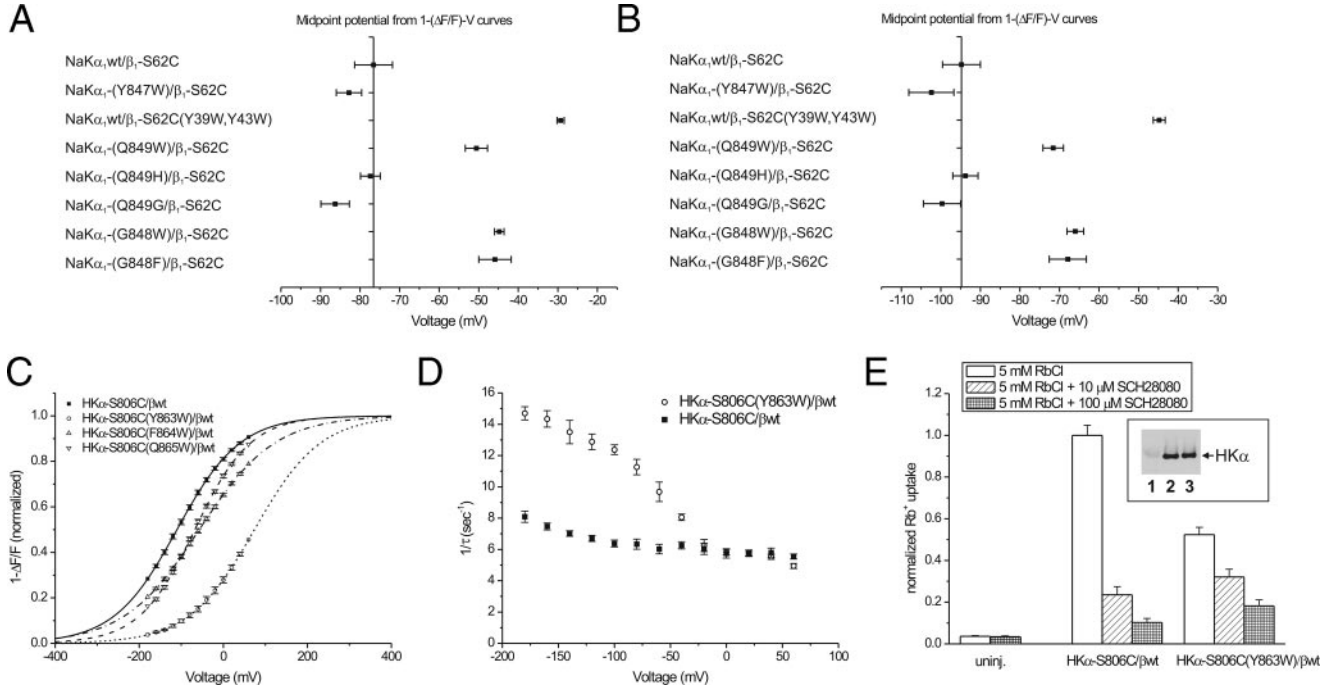

FIGURE 8. **Voltage-dependent E_1P/E_2P distribution of Na,K- and H,K-ATPase α-TMD7 variants.** *A* and *B*, midpoint potentials derived from fits of a Boltzmann function to the voltage-dependent distributions of transported charge *Q* (*A*) or of fluorescence amplitudes $1 - \Delta F/F$ (*B*) for Na,K-ATPase complexes consisting of either the wild type α_1-subunit or various α_1-TMD7 mutants co-expressed with construct β_1-S62C. Data are means ± S.E. of 15–25 oocytes from two to three different oocyte batches normalized to saturating values at −180 mV after subtracting the values for +60 mV. *C*, voltage-dependent E_1P/E_2P distribution of fluorescently labeled H,K-ATPase α-S806C/βwt (■) and three α-TMD7 variants, HKα-S806C(Y863W)/βwt (○), HKα-S806C(F864W)/βwt (△), and HKα-S806C(Q865W)/βwt (▽). Data are means ± S.E. of 15–20 oocytes at pH 5.5 applied to voltage jumps from a holding potential of −40 mV to values between +60 and −180 mV (20-mV increments). A curve resulting from a fit of a Boltzmann function is superimposed (see Table 2 for parameters). Fluorescence amplitudes $1 - \Delta F/F$ were normalized to saturation values from the fits. *D*, reciprocal time constants of voltage jump-induced fluorescence changes for oocytes expressing the H,K-ATPase wild type β-subunit together with either H,K-ATPase HKα-S806C (■) or HKα-S806C(Y863W) (○). Data are means ± S.E. of 14–17 oocytes from two to three different oocyte batches. *E*, Rb^+ uptake of uninjected (*uninj.*) oocytes and oocytes expressing either HKα-S806C/βwt or HKα-S806C(Y863W)/βwt. Rb^+ uptake was determined at pH 5.5 in extracellular Na^+-free solution containing 5 mM RbCl in the absence (*white bars*) or presence of SCH28080 (*hatched bars*, 10 μM; *crossed bars*, 100 μM). Data are means ± S.E., $n = 50–60$ oocytes from four independent experiments normalized to wild type Rb^+ uptake at 5 mM RbCl corresponding to 27.1, 37.9, 29.7, and 48.9 pmol min^{-1}/oocyte. *Inset*, Western blot analysis of isolated plasma membranes from uninjected oocytes (*lane 1*) or oocytes expressing either HKα-S806C/βwt (*lane 2*) or HKα-S806C(Y863W)/βwt (*lane 3*) using anti-H,Kα antibody HK12.18. The equivalent of two oocytes was loaded per lane.

of Gly^{848}. To further clarify this issue, we also investigated the Q849G mutant, which has no bulky side chain but cannot form side chain H-bonds, and the mutant Q849H, whose side chain is well suited to form hydrogen bonds. Of note, although Gln^{849} is rather conserved among most α-subunits, a histidine is found in the corresponding position of the non-gastric H,K-ATPase (Fig. 1*D*), thus possibly indicating a necessity for a hydrogen-bonding side chain in this position. Keeping in mind that mainly the aromatic part and not the hydroxyl group of the β-tyrosines was crucial for the E_2-stabilizing effect (see above), an amino-aromatic interaction to the positively charged or δ^+ amino groups of glutamine or histidine is actually even more likely than classical hydrogen bonding: the side chain of Gln^{849} (or His^{849}) is within 6 Å of the ring centroid of β-Tyr^{39} (Fig. 1*B*) and thus optimally positioned to make van der Waals contact with the δ^- of the π-electrons of tyrosine according to Burley and Petsko (49). This would also allow the formation of an amino-aromatic H-bond as described between the side chain NH_2 of Asn^{44} and Tyr^{35} in bovine pancreatic trypsin inhibitor (50).

Yet the midpoint potentials of Q849H and Q849G were not significantly different from the wild type for both *Q-V* and $(1 - \Delta F/F)$-*V* curves, favoring the idea that Gln^{849} is not directly involved in the interaction to the β-subunit tyrosines because its ability to form hydrogen bonds (or provide δ^+ amino groups for amino-aromatic interactions) apparently does not play a role for the E_1/E_2 steady-state distribution. Therefore, rather the Gly^{848} backbone N-H is the prime candidate for donating an amino-aromatic hydrogen-bond to the phenyl rings of β-Tyr^{39} or β-Tyr^{43} because the centroids of both are within the aforementioned critical distance of 6 Å.

Of note, tryptophan replacement of Tyr^{847} results in *Q-V* and $(1 - \Delta F/F)$-*V* curves with unaltered $V_{0.5}$ values but significantly reduced slope factors, z_q (0.56 instead of ~0.75 for the wild type; see Table 2). Apparently this residue is not relevant for the supposed E_2-specific β-interaction; this seems reasonable because its side chain is not directed toward the β-subunit but rather points toward the cation binding pocket (Fig. 1*B*). This might possibly explain why a parameter is altered (lowered z_q) that reflects electrogenic, hence voltage-dependent properties of the enzyme. The reduced z_q value can be interpreted in terms of a reduced apparent depth of the proposed ion access channel for extracellular Na^+ reverse binding or release (42) as a consequence of the tryptophan replacement. Moreover we determined the apparent affinity for extracellular K^+ by measuring the K^+ dependence of pump current amplitudes and found a significantly higher apparent $K_{½}$ for this mutant (2.6 mM instead of 1.1 mM for the wild type at −40 mV; see supplemental

Fig. 1), indicating that the inserted tryptophan in position 847 also interferes with K^+ binding to the extracellular binding site.

Regarding the H,K-ATPase α-subunit variants, a pronounced positive shift of the $(1 - \Delta F/F)$-V curves was observed for all three investigated variants H,Kα-Y863W, -F864W, and -Q865W (Fig. 8*C*). Surprisingly the most pronounced effect was observed for the Y863W mutant, which shifted the midpoint potential of the E_1/E_2 distribution by about +180 mV toward extremely positive potentials. As shown in Fig. 8*D*, the reciprocal time constants obtained from monoexponential fitting to the fluorescence changes were almost increased 2-fold for the H,Kα-Y863W mutant compared with the wild type at very negative potentials, whereas there was no significant difference at positive potentials. This can be interpreted as an acceleration of the backward rate constant k_{-1} (Fig. 7) without concomitant changes in $k_{1,}$ thus resulting in an E_1 shift of the E_1P/E_2P conformational distribution. Notably, these kinetic alterations are very similar to those observed for the Na,K-ATPase β_1-S62C(Y39W,Y43W) variant (Fig. 3, *C* and *D*). Again the E_1 shift is also reflected by a reduced SCH28080 sensitivity of the Y863W mutant compared with the HKαS806C reference construct in the presence of 5 mM RbCl and 10 or 100 μM SCH28080, respectively (Fig. 8*E*). Moreover the Rb^+ uptake of the H,Kα-Y863W variant was reduced to about 50% of the wild type uptake at 5 mM RbCl (Fig. 8*E*), but this could not be attributed to changes in the apparent Rb^+ affinity (supplemental Table 1) or a reduced cell surface delivery (Fig. 8*E*, *inset*). Therefore, the turnover number of the mutant enzyme is apparently affected too.

The finding that the most pronounced effects of tryptophan replacements in the H,K-ATPase TMD7 occurred in position Tyr^{863} (and not Phe^{864}, corresponding to NaK-Gly^{848}) indicates that the location of the interaction interface on the α-subunit might be different for H,K- and Na,K-ATPase enzymes because the corresponding residue Tyr^{847} of the sodium pump did not seem important for the E_1/E_2 distribution. Furthermore even the mechanism of the interaction may be different for the two ATPases: the side chains of Tyr^{863} and Phe^{864} in the H,K-ATPase TMD7 probably exert their E_2-stabilizing effect rather by aromatic-aromatic interactions (π-stacking; see Ref. 51) with Tyr^{44} and Tyr^{48} in the β-TMD. Yet despite the huge effects on the E_1P/E_2P conformational equilibrium, none of these H,K-ATPase mutations exhibited altered apparent affinities for extracellular Rb^+ (see supplemental Table 1).

This apparently contradicts findings obtained for the β-(Y44W,Y48W) mutant, which showed a less pronounced E_1 shift of the $(1 - \Delta F/F)$-V curve but exhibited a substantially reduced apparent affinity for extracellular Rb^+. However, the VCF data for this β-subunit mutant should be considered with caution because the observed fluorescence changes were only about 10% compared with those obtained for wild type or mutant α-subunit H,K-ATPases. The unaffected maximal Rb^+ uptake per cell at saturating Rb^+ concentrations (see legend to Fig. 5, *B* and *C*) indicates that the lower fluorescence amplitudes are not due to a reduced cell surface delivery of the β-(Y44W,Y48W) mutant. This interpretation was also confirmed by Western blots of isolated plasma membrane protein fractions (see supplemental Fig. 2) that show that the amounts of protein at the cell surface are very similar. Therefore, we suggest instead that the β-(Y44W,Y48W) mutant has an extremely high preference for the E_1P state (as inferred from the dramatic Rb^+ affinity changes and the reduced SCH28080 sensitivity), which prevents the enzymes from being completely shifted toward E_2P by stepping to positive potentials. Because only relative changes in the conformational distribution are reported by the VCF technique the weak fluorescence signals observed for the β-(Y44W,Y48W) variant enzyme indicate that most likely an incomplete E_1P/E_2P conformational transition is monitored; thus the absolute E_1 shift for the mutant enzyme might be underestimated.

Physiological Relevance of the E_2-stabilizing Effect of the β-Subunits for Na,K- and Gastric H,K-ATPase Activity in Situ—In this study, we demonstrated a common E_2-stabilizing effect of conserved Tyr residues in the β-subunit TMD for oligomeric Na,K- and H,K-ATPase and also provided insights into the structural determinants of the E_2-specific interaction underlying this stabilization. The functional significance is less pronounced for the Na,K-ATPase where an E_1-shifted equilibrium caused by the TMD mutations only involved minor changes in the apparent ion affinities such that no substantial effect on the transport rate of the sodium pump is exerted under physiological conditions.

In contrast, the E_1 preference caused by the homologous β-(Y44W,Y48W) mutation in gastric H,K-ATPase has serious effects on cation affinities: because the apparent $K_{½}$ for extracellular K^+ (Rb^+) was shown to be more than 4-fold increased (in the presence of extracellular Na^+), the mutated H,K-ATPase is not able to operate at maximal turnover *in situ*. Usually luminal K^+ concentrations are low at least before K^+-secreting KCNQ1/KCNE2 potassium channels in the luminal parietal cell membrane are activated by acidification to about pH 3.5 (52, 53), a process that itself requires H,K-ATPase activity. Moreover even an increase of the potassium concentration in the stomach lumen to saturating levels of about 15 mM (34), *e.g.* by a K^+-rich diet or as a result of sustained KCNQ1/KCNE2 activity, would not help much because the enhanced H^+ rebinding of the mutant would still be fatal for efficient H^+ secretion (as demonstrated at 20 mM RbCl; Fig. 6). For the H,K-ATPase it is of pivotal importance that protons can be effectively released from the extracellular binding sites even at pH values as low as 2. Because this requires pK_a changes of 5–6 orders of magnitude during the E_1P to E_2P transition, the relative destabilization of the E_2 state in favor of E_1, which is characteristic for the mutant, most likely results in a substantially lowered efficiency of luminal proton release. In the stomach, the combination of both decreased apparent K^+ affinity and reduced proton release is expected to suppress H,K-ATPase activity dramatically, thus rendering the mutant enzyme unable to sustain sufficiently low pH levels required for digestion and antibacterial purposes. Despite the observed unaffected Rb^+ affinity, the phenotype resulting from the H,Kα-Y863W mutation would also result in a significant reduction of H^+ secretion in the stomach because the turnover number (v_{max}) of this mutant is about 2-fold lowered. Therefore, the E_2 stabilization mediated by E_2-specific intersubunit interactions between two conserved tyrosines in the Na,K- or H,K-ATPase β-TMD and

TMD7 of the respective catalytic α-subunit, which is the main finding of this study, is of high functional significance for the gastric H,K-ATPase *in situ*.

Acknowledgments—We thank Janna Lustig for technical assistance and Dr. Klaus Hartung for numerous helpful discussions and suggestions.

REFERENCES

1. Palmgren, M. G., and Axelsen, K. B. (1998) *Biochim. Biophys. Acta* **1365,** 37–45
2. Axelsen, K. B., and Palmgren, M. G. (1998) *J. Mol. Evol.* **46,** 84–101
3. Shull, G. E., and Lingrel, J. B. (1986) *J. Biol. Chem.* **261,** 16788–16791
4. Altendorf, K., Gassel, M., Puppe, W., Mollenkamp, T., Zeeck, A., Boddien, C., Fendler, K., Bamberg, E., and Drose, S. (1998) *Acta Physiol. Scand. Suppl.* **643,** 137–146
5. Gottardi, C. J., and Caplan, M. J. (1993) *J. Biol. Chem.* **268,** 14342–14347
6. McDonough, A. A., Geering, K., and Farley, R. A. (1990) *FASEB J.* **4,** 1598–1605
7. Geering, K. (1991) *FEBS Lett.* **285,** 189–193
8. Geering, K. (2001) *J. Bioenerg. Biomembr.* **33,** 425–438
9. Noguchi, S., Mishina, M., Kawamura, M., and Numa, S. (1987) *FEBS Lett.* **225,** 27–32
10. Jaisser, F., Jaunin, P., Geering, K., Rossier, B. C., and Horisberger, J. D. (1994) *J. Gen. Physiol.* **103,** 605–623
11. Crambert, G., Hasler, U., Beggah, A. T., Yu, C., Modyanov, N. N., Horisberger, J. D., Lelievre, L., and Geering, K. (2000) *J. Biol. Chem.* **275,** 1976–1986
12. Horisberger, J. D., Jaunin, P., Reuben, M. A., Lasater, L. S., Chow, D. C., Forte, J. G., Sachs, G., Rossier, B. C., and Geering, K. (1991) *J. Biol. Chem.* **266,** 19131–19134
13. Eakle, K. A., Kim, K. S., Kabalin, M. A., and Farley, R. A. (1992) *Proc. Natl. Acad. Sci. U. S. A.* **89,** 2834–2838
14. Kawamura, M., Ohmizo, K., Morohashi, M., and Nagano, K. (1985) *Biochim. Biophys. Acta* **821,** 115–120
15. Lutsenko, S., and Kaplan, J. H. (1993) *Biochemistry* **32,** 6737–6743
16. Chow, D. C., Browning, C. M., and Forte, J. G. (1992) *Am. J. Physiol.* **263,** C39–C46
17. Jaunin, P., Jaisser, F., Beggah, A. T., Takeyasu, K., Mangeat, P., Rossier, B. C., Horisberger, J. D., and Geering, K. (1993) *J. Cell Biol.* **123,** 1751–1759
18. Eakle, K. A., Kabalin, M. A., Wang, S. G., and Farley, R. A. (1994) *J. Biol. Chem.* **269,** 6550–6557
19. Hasler, U., Wang, X., Crambert, G., Beguin, P., Jaisser, F., Horisberger, J. D., and Geering, K. (1998) *J. Biol. Chem.* **273,** 30826–30835
20. Morth, J. P., Pedersen, B. P., Toustrup-Jensen, M. S., Sorensen, T. L., Petersen, J., Andersen, J. P., Vilsen, B., and Nissen, P. (2007) *Nature* **450,** 1043–1049
21. Geering, K., Beggah, A., Good, P., Girardet, S., Roy, S., Schaer, D., and Jaunin, P. (1996) *J. Cell Biol.* **133,** 1193–1204
22. Abriel, H., Hasler, U., Geering, K., and Horisberger, J. D. (1999) *Biochim. Biophys. Acta* **1418,** 85–96
23. Chow, D. C., and Forte, J. G. (1993) *Am. J. Physiol.* **265,** C1562–C1570
24. Hasler, U., Greasley, P. J., von Heijne, G., and Geering, K. (2000) *J. Biol. Chem.* **275,** 29011–29022
25. Hasler, U., Crambert, G., Horisberger, J. D., and Geering, K. (2001) *J. Biol. Chem.* **276,** 16356–16364
26. Helmich-de Jong, M. L., van Emst-de Vries, S. E., De Pont, J. J., Schuurmans Stekhoven, F. M., and Bonting, S. L. (1985) *Biochim. Biophys. Acta* **821,** 377–383
27. Geibel, S., Kaplan, J. H., Bamberg, E., and Friedrich, T. (2003) *Proc. Natl. Acad. Sci. U. S. A.* **100,** 964–969
28. Dempski, R. E., Friedrich, T., and Bamberg, E. (2005) *J. Gen. Physiol.* **125,** 505–520
29. Geibel, S., Zimmermann, D., Zifarelli, G., Becker, A., Koenderink, J. B., Hu, Y. K., Kaplan, J. H., Friedrich, T., and Bamberg, E. (2003) *Ann. N. Y. Acad. Sci.* **986,** 31–38
30. Dürr, K. L., Tavraz, N. N., Zimmermann, D., Bamberg, E., and Friedrich, T. (2008) *Biochemistry* **47,** 4288–4297
31. Hu, Y. K., and Kaplan, J. H. (2000) *J. Biol. Chem.* **275,** 19185–19191
32. Price, E. M., and Lingrel, J. B. (1988) *Biochemistry* **27,** 8400–8408
33. Lorenz, C., Pusch, M., and Jentsch, T. J. (1996) *Proc. Natl. Acad. Sci. U. S. A.* **92,** 13362–13366
34. Sachs, G., Shin, J. M., Vagin, O., Lambrecht, N., Yakubov, I., and Munson, K. (2007) *J. Clin. Gastroenterol.* **41,** Suppl. 2, S226–S242
35. Kamsteeg, E. J., and Deen, P. M. (2000) *Am. J. Physiol.* **279,** F778–F784
36. Kamsteeg, E. J., and Deen, P. M. (2001) *Biochem. Biophys. Res. Commun.* **282,** 683–690
37. Laemmli, U. K. (1970) *Nature* **227,** 680–685
38. Rakowski, R. F. (1993) *J. Gen. Physiol.* **101,** 117–144
39. Jaisser, F., Horisberger, J. D., Geering, K., and Rossier, B. C. (1993) *J. Cell Biol.* **123,** 1421–1429
40. Kaplan, J. H., and Hollis, R. J. (1980) *Nature* **288,** 587–589
41. Kaplan, J. H. (1982) *J. Gen. Physiol.* **80,** 915–937
42. Sagar, A., and Rakowski, R. F. (1994) *J. Gen. Physiol.* **103,** 869–893
43. Ray, T. K., and Nandi, J. (1985) *FEBS Lett.* **185,** 24–28
44. Polvani, C., Sachs, G., and Blostein, R. (1989) *J. Biol. Chem.* **264,** 17854–17859
45. Rabon, E. C., Bassilian, S., Sachs, G., and Karlish, S. J. (1990) *J. Biol. Chem.* **265,** 19594–19599
46. Swarts, H. G., Klaassen, C. H., Schuurmans Stekhoven, F. M., and De Pont, J. J. (1995) *J. Biol. Chem.* **270,** 7890–7895
47. Wallmark, B., Briving, C., Fryklund, J., Munson, K., Jackson, R., Mendlein, J., Rabon, E., and Sachs, G. (1987) *J. Biol. Chem.* **262,** 2077–2084
48. Lorentzon, P., Eklundh, B., Brandstrom, A., and Wallmark, B. (1985) *Biochim. Biophys. Acta* **817,** 25–32
49. Burley, S. K., and Petsko, G. A. (1986) *FEBS Lett.* **203,** 139–143
50. Tüchsen, E., and Woodward, C. (1987) *Biochemistry* **26,** 1918–1925
51. Burley, S. K., and Petsko, G. A. (1985) *Science* **229,** 23–28
52. Grahammer, F., Herling, A. W., Lang, H. J., Schmitt-Graff, A., Wittekindt, O. H., Nitschke, R., Bleich, M., Barhanin, J., and Warth, R. (2001) *Gastroenterology* **120,** 1363–1371
53. Heitzmann, D., Grahammer, F., von Hahn, T., Schmitt-Graff, A., Romeo, E., Nitschke, R., Gerlach, U., Lang, H. J., Verrey, F., Barhanin, J., and Warth, R. (2004) *J. Physiol.* **561,** 547–557